

FIG. 5. The microstructure of a pure bismuth specimen tested to failure at atmospheric pressure showing: (a) Cracks formed by the intersection of twins with grain boundaries (75 $\times$ , Unetched, Polarized Light), and (b) Twin-crack pairs felt to nucleate below the plane of polish by the mechanism outlined in Fig. 6. (100 $\times$ , Unetched, Polarized Light).

observed immediately behind the tensile fracture surface as seen in Fig. 7(a). Finally at pressures above the BDTP, cleavage was suppressed and the specimens failed by rupture, (Fig. 7b). The evidence of mechanical twins is less and even in view of the large plastic strains, the grains are equiaxed. This is indicative that the high strains were sufficient to cause post test recrystallization prior to metallographic preparation.

#### *Tin-bismuth alloys*

The trend in ductility exhibited by various Sn-Bi alloys compositions at atmospheric pressure and the variation in transition pressure of these compositions is shown in Fig. 8. Ductility is seen to be a maximum

for pure tin and for near-eutectic compositions with small Bi additions severely lowering the ductility of the high Sn alloys. Comparison of the two curves shows a direct relationship to exist between the effects of pressure and composition on ductility. Those areas having high ductility (pure Sn and near-eutectic compositions) correspond to the low transition pressures, and compositions having a low inherent ductility required a higher value of superimposed hydrostatic pressure in order to fail by rupture.

#### *90 per cent Sn-bal Bi alloy*

For specimens of 90 per cent Sn-bal Bi tested to failure at atmospheric pressure, failure occurs along a section nominally perpendicular to the longitudinal axis; as the pressure increases, the appearance of the fracture corresponds to failure by ductile rupture. At atmospheric and low values of superimposed hydrostatic pressure, cracks are seen to originate along the interface between Bi particles and the Sn matrix (Fig. 9), whereas particle-matrix separation is not seen in specimens tested closer to the BDTP. Numerous voids, having the general shape of micro-cracks, were seen in areas adjacent to the fracture surface at atmospheric and near-atmospheric pressures (Fig. 10a), but not at pressures approaching the BDTP (Fig. 10b). At atmospheric and low pressures, the mode of fracture appears to be mixed, with evidence for the occurrence of both cleavage at interphase boundaries and ductile tearing present as seen in Fig. 11(a). As the superimposed hydrostatic pressure approaches the BDTP, the fracture surface gradually converts to a dimpled structure, Fig. 11(b), with these dimples decreasing in size at the BDTP as shown in Fig. 11(c).

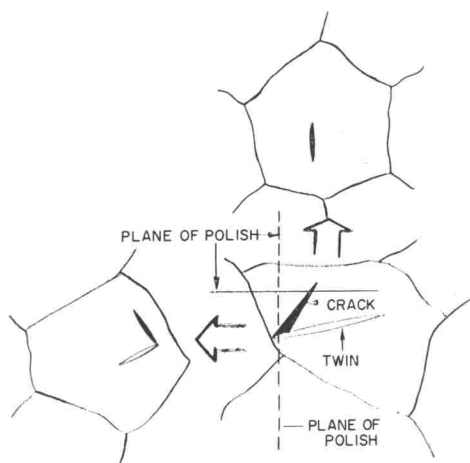


FIG. 6. A schematic representation of the appearance of cracks without metallographically observed obvious means of nucleation. The plane of polish intersects the crack above the point of nucleation, and results in the structures seen in Fig. 5(b).

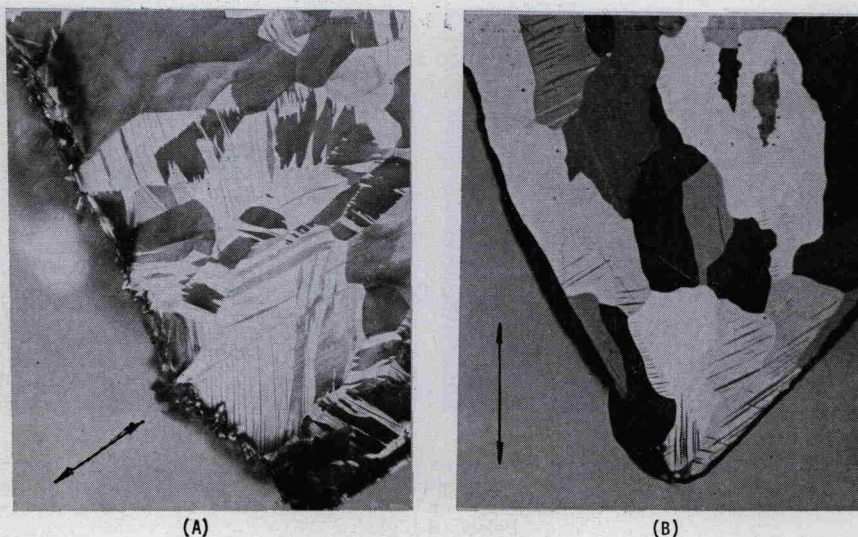


FIG. 7. The microstructure of pure bismuth specimens which fractured at superimposed hydrostatic pressures of: (a)  $6.3 \times 10^8 \text{ N/m}^2$ , and (b)  $14.2 \times 10^8 \text{ N/m}^2$ .  $50\times$ , Unetched, Polarized Light. Tensile axis indicated by arrows.

#### 75 per cent Sn-bal Bi alloy

As compared to the former alloy, this alloy contains a higher density of bismuth particles along the Sn grain boundaries and crystallographic planes. This results in a higher microcrack density and a greater propensity towards cleavage fracture. The changes with pressure are otherwise effectively the same.

#### 42 per cent Sn-bal Bi alloy

This near eutectic alloy composition was seen to contain voids in the interior of the specimen behind the fracture surface when tested to failure at atmospheric pressure (Fig. 12a). Of interest is the shape of the voids; the "V" shape indicates failure by shear,

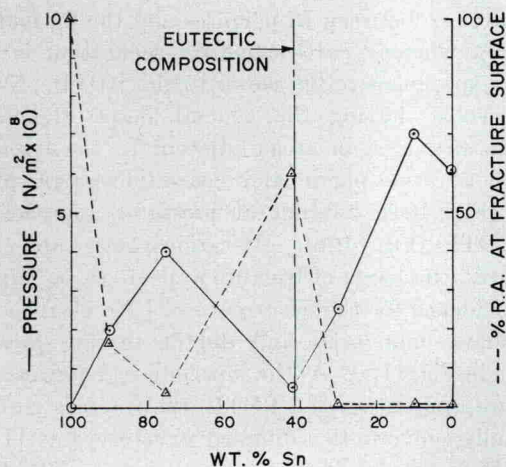


FIG. 8. The variation in ductility and ductility transition pressure as a function of composition.

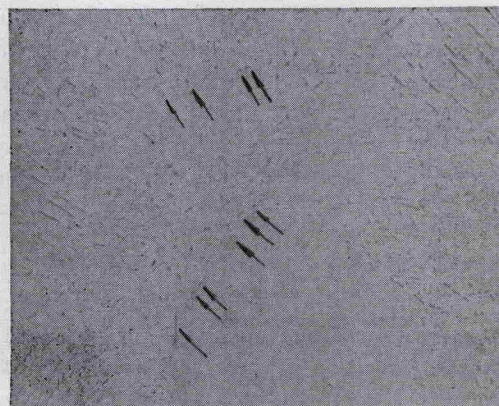


FIG. 9(a). The microstructure of a 90% Sn-bal Bi specimen where pressure at fracture equalled  $0.5 \times 10^8 \text{ N/m}^2$ . Note the grain size and cracks between matrix and particles straddling grain boundaries.  $500\times$ , Unetched.



FIG. 9(b). The microstructure of a 90% Sn-bal Bi specimen where pressure at fracture equalled  $1.55 \times 10^8 \text{ N/m}^2$ . Note the smaller grain size than that shown by Fig. 9 (a) and lack of particle-matrix separation.  $500\times$ , Unetched.